

This is a self-archived version of an original article. This version may differ from the original in pagination and typographic details.

Author(s): Feng, Tai-Fu

Title: The two-loop gluino's corrections on the inclusive $b \rightarrow s \gamma$ decay in the CP violation MSSM with large $\tan \beta$

Year: 2004

Version: Published version

Copyright: © 2004 American Physical Society.

Rights: In Copyright

Rights url: <http://rightsstatements.org/page/InC/1.0/?language=en>

Please cite the original version:

Feng, T.-F. (2004). The two-loop gluino's corrections on the inclusive $b \rightarrow s \gamma$ decay in the CP violation MSSM with large $\tan \beta$. Physical Review D, 70(9), 1.
<https://doi.org/10.1103/PhysRevD.70.096012>

Two-loop gluino corrections to the inclusive decay $B \rightarrow X_s \gamma$ in the CP violating MSSM with large $\tan\beta$

Tai-Fu Feng

Department of Physics, 40014 University of Jyväskylä, Finland
(Received 20 May 2004; published 24 November 2004)

We investigate two-loop gluino corrections to the effective Lagrangian for $b \rightarrow s + \gamma(g)$ in the minimal supersymmetric extension of the standard model (MSSM) at large $\tan\beta$, including the contributions in which quark flavor change is mediated by charginos. Using the translation invariance of loop momenta and the Ward-Takahashi identities that are required by the $SU(3)_c \times U(1)_{em}$ gauge invariance, we simplify our expressions to concise forms. As an example, we discuss two-loop gluino corrections to the CP asymmetry of inclusive $B \rightarrow X_s \gamma$ decay in CP violating MSSM.

DOI: 10.1103/PhysRevD.70.096012

PACS numbers: 11.30.Er, 12.60.Jv, 14.80.Cp

I. INTRODUCTION

The measurements of the branching ratios at CLEO, ALEPH, and BELLE [1] give the combined result

$$BR(B \rightarrow X_s \gamma) = (3.11 \pm 0.42 \pm 0.21) \times 10^{-4}, \quad (1)$$

which agrees with the next-to-leading order (NLO) standard model (SM) prediction [2]

$$BR(B \rightarrow X_s \gamma) = (3.29 \pm 0.33) \times 10^{-4}. \quad (2)$$

Good agreement between the experiment and the theoretical prediction of the SM implies that the new physics scale should lie well above the electroweak (EW) scale. The systematic analysis of new physics corrections to $B \rightarrow X_s \gamma$ up to two-loop order can help us understand where the new physics scale sets in, and the distribution of new physical particle masses around this scale. In principle, the two-loop corrections can be large when some additional parameters are involved at this perturbation order beside the parameters appearing in one-loop results. In other words, including the two-loop contributions one can obtain a more exact constraint on the new physics parameter space from the present experimental results.

Beside the Cabibbo-Kobayashi-Maskawa (CKM) mechanism, the soft breaking terms provide a new source of CP and flavor violation in the minimal supersymmetric standard model (MSSM). Those CP violating phases can affect the important observables in the mixing of Higgs bosons [3], the lepton and neutron's electric dipole moments (EDMs) [4,5], lepton polarization asymmetries in the semileptonic decays [6], the production of P -wave charmonium and bottomonium [7], and CP violation in rare B decays and in $B^0 \bar{B}^0$ mixing [8]. At present, the strictest constraints on those CP violation phases originate from the lepton and neutron's EDMs. Nevertheless, if we invoke a cancellation mechanism among different supersymmetric contributions [4], or choose the fermions of the first generation heavy enough [5], the loop inducing lepton and neutron's EDMs bound the argument of the μ

parameter to be $\leq \pi/(5 \tan\beta)$, leaving no constraints on the other explicitly CP violating phases.

The supersymmetry models at large $\tan\beta$ are implied by grand unified theories, where the unification of up- and down-type quark Yukawa couplings is made [9]. From the technical viewpoint, the dominant contributions to the relevant effective Lagrangian are the terms proportional to $(\tan\beta)^n$ ($n = 1, 2, \dots$) in a large $\tan\beta$ scenario. This will simplify our two-loop analysis drastically since we just keep those terms enhanced by $\tan\beta$.

Assuming no additional sources of flavor violation other than the CKM matrix elements, the authors of [10] present an exact analysis of two-loop gluino corrections to the rare decay $b \rightarrow s + \gamma(g)$ in which quark flavor change is mediated by the charged Higgs in CP conserving MSSM at large $\tan\beta$. They also compare their exact result with that originating from the heavy mass expansion (HME) approximation [11]. Although the HME result approximates the exact two-loop analysis adequately when the supersymmetry energy scale is high enough, their analysis implies that the difference between the HME approximation and exact calculation is obvious in some parameter space of the MSSM. However, they do not consider the case in which quark flavor change is mediated by the charginos (the super partners of the charged Higgs and W bosons). In fact, we cannot provide any strong reason to ignore the contribution from the diagrams in which quark flavor change is induced by the charginos, even within large $\tan\beta$ scenarios. In this work, we present a complete analysis on the two-loop gluino corrections to the rare transitions $b \rightarrow s + \gamma(g)$ by including the contributions of those diagrams where quark flavor change is mediated by charginos in the framework of CP violating MSSM at large $\tan\beta$. Furthermore, we also simplify our expressions to concise forms through loop momentum invariance and the Ward-Takahashi identities (WTIs) that are required by the $SU(3)_c \times U(1)_{em}$ gauge invariance.

The paper is organized as follows. In Sec. II, we give all the diagrams needed to evaluate the $O(\alpha_s \tan\beta)$ con-

tributions to the Wilson coefficients C_7 and C_8 entering the branching ratio $BR(B \rightarrow X_s \gamma)$. The corresponding Wilson coefficients at the matching EW scale μ_{EW} are also presented there. We apply the effective Lagrangian to the rare decay $B \rightarrow X_s \gamma$ in Sec. III. By the numerical method, we show the two-loop corrections on the CP asymmetry for the process. Our conclusion is given in Sec. IV, and some long formulas are collected in the Appendices.

II. THE WILSON COEFFICIENTS FROM THE TWO-LOOP DIAGRAMS

In this section, we derive the relevant Wilson coefficients for the partonic decay $b \rightarrow s \gamma$ including two-loop gluino corrections. In a conventional form, the effective Hamiltonian is written as

$$H_{\text{eff}} = -\frac{4G_F}{\sqrt{2}} V_{ts}^* V_{tb} \sum_{i=1}^8 C_i(\mu) \mathcal{O}_i, \quad (3)$$

where V is the CKM matrix. The definitions of the magnetic and chromomagnetic dipole operators are

$$\begin{aligned} \mathcal{O}_7 &= \frac{e}{(4\pi)^2} m_b(\mu) \bar{s}_L \sigma^{\mu\nu} b_R F_{\mu\nu}, \\ \mathcal{O}_8 &= \frac{g_s}{(4\pi)^2} m_b(\mu) \bar{s}_L T^a \sigma^{\mu\nu} b_R G_{\mu\nu}^a, \end{aligned} \quad (4)$$

where $F_{\mu\nu}$ and $G_{\mu\nu}^a$ are the field strengths of the photon and gluon, respectively, and T^a ($a = 1, \dots, 8$) are $SU(3)_c$ generators. In addition, e and g_s represent the EW and strong couplings, respectively. The other operators \mathcal{O}_i ($i = 1, \dots, 6$) are defined in [12].

In the framework of CP violating MSSM, the one-loop analysis on the CP asymmetry of inclusive $B \rightarrow X_s \gamma$ decay has been presented elsewhere [9]. The two-loop gluino diagrams, contributing at $\mathcal{O}(\alpha_s \tan\beta)$ to the Wilson coefficients of the magnetic and chromomagnetic dipole operators, are obtained from the self-energy diagrams Fig. 1(a) and 1(b) by attaching a photon or gluon in all possible ways. The calculation of the Wilson coefficients for the operators in Eq. (4) at two-loop order is more challenging than that at one-loop order. Before we give those Wilson coefficient expressions explicitly, we state first the concrete steps required to obtain the coefficients from those two-loop diagrams.

(i) After writing the amplitudes of those two-loop triangle diagrams, we expand them in powers of external momenta to the second order.

(ii) The even rank tensors in loop momenta can be replaced as follows:

$$\begin{aligned} \int \frac{d^D q_1}{(2\pi)^D} \frac{d^D q_2}{(2\pi)^D} \frac{q_{1\mu} q_{1\nu} q_{1\mu} q_{2\nu}}{\mathcal{D}_0} &\rightarrow \frac{g_{\mu\nu}}{D} \int \frac{d^D q_1}{(2\pi)^D} \frac{d^D q_2}{(2\pi)^D} \frac{q_1^2 q_2^2}{\mathcal{D}_0}, \\ \int \frac{d^D q_1}{(2\pi)^D} \frac{d^D q_2}{(2\pi)^D} \frac{q_{1\mu} q_{1\nu} q_{1\rho} q_{1\sigma} q_{1\mu} q_{1\nu} q_{1\rho} q_{2\sigma}}{\mathcal{D}_0} &\rightarrow \frac{T_{\mu\nu\rho\sigma}}{D(D+2)} \int \frac{d^D q_1}{(2\pi)^D} \frac{d^D q_2}{(2\pi)^D} \frac{q_1^4 q_2^2 (q_1 \cdot q_2)}{\mathcal{D}_0}, \\ \int \frac{d^D q_1}{(2\pi)^D} \frac{d^D q_2}{(2\pi)^D} \frac{q_{1\mu} q_{1\nu} q_{2\rho} q_{2\sigma}}{\mathcal{D}_0} &\rightarrow \int \frac{d^D q_1}{(2\pi)^D} \frac{d^D q_2}{(2\pi)^D} \frac{1}{\mathcal{D}_0} \\ &\times \left(\frac{D(q_1 \cdot q_2)^2 - q_1^2 q_2^2}{D(D-1)(D+2)} T_{\mu\nu\rho\sigma} - \frac{(q_1 \cdot q_2)^2 - q_1^2 q_2^2}{D(D-1)} g_{\mu\nu} g_{\rho\sigma} \right), \end{aligned} \quad (5)$$

where D is the time-space dimension, $T_{\mu\nu\rho\sigma} = g_{\mu\nu} g_{\rho\sigma} + g_{\mu\rho} g_{\nu\sigma} + g_{\mu\sigma} g_{\nu\rho}$, and $\mathcal{D}_0 = [(q_2 - q_1)^2 - m_0^2](q_1^2 - m_a^2) \times (q_2^2 - m_a^2)$. The odd rank tensors in loop momenta can be dropped since the integrations are symmetric under the transformation $q_{1,2} \rightarrow -q_{1,2}$. Here, we only retain the simplest two-loop propagator composition $1/\mathcal{D}_0$ which corresponds to the two-loop vacuum diagram (Fig. 2). Any complicated composition of two-loop propagators can be expressed as the linear combination of the simplest one $1/\mathcal{D}_0$ by use of the obvious decomposition formula

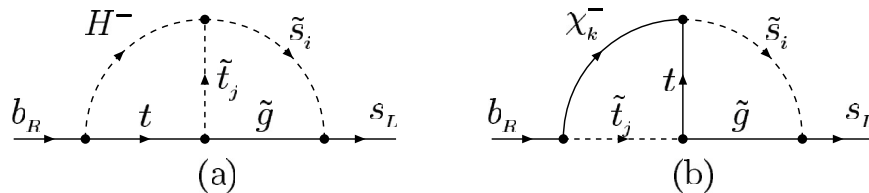


FIG. 1. The self-energy diagrams which lead to the magnetic and chromomagnetic operators in the MSSM, the corresponding triangle diagrams are obtained by attaching a photon or gluon in all possible ways.

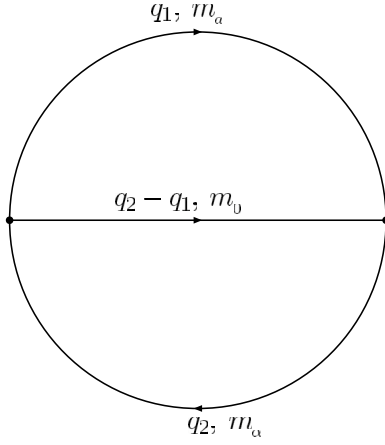


FIG. 2. The two-loop vacuum diagram with momenta and masses as in Eq. (5).

$$\frac{1}{(Q^2 - m_A^2)(Q^2 - m_B^2)} = \frac{1}{m_A^2 - m_B^2} \left(\frac{1}{Q^2 - m_A^2} - \frac{1}{Q^2 - m_B^2} \right), \quad (6)$$

with $Q = q_1, q_2$, or $q_2 - q_1$. As an example, we apply

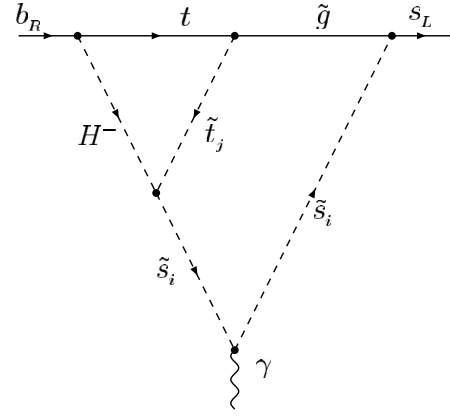


FIG. 3. A triangle diagram in which the external photon is attached to squark \tilde{s}_i .

the above steps to the triangle diagram in which an external photon is attached to the internal squark \tilde{s}_i line (Fig. 3). After expanding the corresponding amplitude in powers of external momenta to the second order, we have

$$\begin{aligned} iA_{(1)\mu}^\gamma(p, k) = & -i \frac{4}{3} e_d g_s^2 \frac{e^3}{m_w s_w^2} V_{ts}^* V_{tb} \left(\frac{m_b}{m_w} \tan \beta \right) (Z_{\tilde{s}})_{2,i} (Z_{\tilde{s}}^\dagger)_{i,2} \left[|\mu| m_t e^{-i\theta_\mu} (Z_{\tilde{t}})_{2,j} + \frac{\sqrt{2} m_w s_w \mathbf{A}_s}{e} (Z_{\tilde{t}})_{1,j} \right] \\ & \times \int \frac{d^D q_1}{(2\pi)^D} \frac{d^D q_2}{(2\pi)^D} \frac{1}{\mathcal{D}_H(q_1^2 - m_{\tilde{s}_i}^2)} \left\{ 1 + \frac{2q_1 \cdot (2p + k)}{q_1^2 - m_{\tilde{s}_i}^2} + \frac{2q_2 \cdot p}{q_2^2 - m_{H^+}^2} \right\} \\ & \times \{ (Z_{\tilde{t}}^\dagger)_{j,3} \not{q}_1 \not{q}_2 (2q_1 - 2p - k)_\mu \omega_+ - m_t |m_3| e^{i\theta_3} (Z_{\tilde{t}}^\dagger)_{j,2} (2q_1 - 2p - k)_\mu \omega_+ \}, \end{aligned} \quad (7)$$

where p, k represent the incoming momenta of the external quark b and photon, respectively, $\mathcal{D}_H = [(q_2 - q_1)^2 - m_{\tilde{t}_j}^2](q_1^2 - |m_3|^2)(q_1^2 - m_{\tilde{s}_i}^2)(q_2^2 - m_{\tilde{t}_j}^2)(q_2^2 - m_{H^+}^2)$ ($i, j = 1, 2$) and $e_d = -1/3$. $Z_{\tilde{q}}$ ($q = u, d, \dots, t$) are the mixing matrices of scalar quarks, and \mathbf{A}_q are the corresponding trilinear soft breaking parameters. Furthermore, $\theta_{3,\mu}$ denote the CP phases of the $SU(3)_c$ gaugino mass and of the μ parameter, respectively. Since the quark mass m_b from the bottom quark Yukawa coupling is same order as the external momenta p, k in magnitude, we just expand the propagators in powers of external momenta to the first order. In the soft breaking potential, the CP phase θ_3 is contained in the gluino mass terms

$$|m_3| e^{i\theta_3} \sum_a \lambda_G^a \lambda_G^a + |m_3| e^{-i\theta_3} \sum_a \bar{\lambda}_G^a \bar{\lambda}_G^a, \quad (8)$$

where λ_G^a ($a = 1, \dots, 8$) denote the gluino fields in two-component Majorana spinors. With the redefinition of gluino fields

$$\lambda_G^a \rightarrow \lambda_G^a e^{-(i/2)\theta_3}, \quad \bar{\lambda}_G^a \rightarrow \bar{\lambda}_G^a e^{(i/2)\theta_3}, \quad (9)$$

the mass terms are transformed into

$$|m_3| \sum_a \bar{\tilde{g}}^a \tilde{g}^a \quad (10)$$

with the four-component Majorana spinors

$$\tilde{g}^a = \begin{pmatrix} \lambda_G^a \\ \bar{\lambda}_G^a \end{pmatrix}. \quad (11)$$

Correspondingly, the CP phase θ_3 is transferred from the mass terms to the quark-squark-gluino vertex which is given by [13]

$$\begin{aligned} -\mathcal{L}_{\tilde{q}\tilde{q}\tilde{g}} = & \sqrt{2} g_s T_{\alpha\beta}^a \sum_q [-e^{-(i/2)\theta_3} (Z_{\tilde{q}})_{2,i} \bar{q}^\alpha \omega_- \tilde{g}_a \tilde{q}_i^\beta \\ & + e^{(i/2)\theta_3} (Z_{\tilde{q}})_{1,i} \bar{q}^\alpha \omega_+ \tilde{g}_a \tilde{q}_i^\beta] + \text{H.c.} \end{aligned} \quad (12)$$

Here, $\alpha, \beta = 1, 2, 3$ are quark and squark color indices, and $\omega_\pm = \frac{1 \pm \gamma_5}{2}$. This is the reason why there is a $|m_3|$ rather than m_3 in the gluino propagator. Using Eqs. (5) and (6), the amplitude of Fig. 3 is finally formulated as

$$\begin{aligned}
iA_{(1)\mu}^\gamma(p, k) = & -i\frac{4}{3}e_d g_s^2 \frac{e^3}{m_w s_w^2} V_{ts}^* V_{tb} \left(\frac{m_b}{m_w} \tan\beta \right) (Z_s^\dagger)_{2,i} (Z_s^\dagger)_{i,2} \left[|\mu| m_t e^{-i\theta_\mu} (Z_t)_{2,j} + \frac{\sqrt{2} m_w s_w \mathbf{A}_s}{e} (Z_t)_{1,j} \right] \\
& \times \int \frac{d^D q_1}{(2\pi)^D} \frac{d^D q_2}{(2\pi)^D} \frac{1}{\mathcal{D}_H(q_1^2 - m_{\tilde{s}_i}^2)} \left\{ (Z_t^\dagger)_{j,3} \left[\frac{4}{D} \frac{q_1^2 q_1 \cdot q_2}{q_1^2 - m_{\tilde{s}_i}^2} (2p+k)_\mu \omega_+ - q_1 \cdot q_2 (2p+k)_\mu \omega_+ + \frac{4}{q_2^2 - m_{H^+}^2} \right. \right. \\
& \times \left(\frac{D(q_1 \cdot q_2)^2 - q_1^2 q_2^2}{D(D-1)} p_\mu \omega_+ - \frac{(q_1 \cdot q_2)^2 - q_1^2 q_2^2}{D(D-1)} \gamma_\mu \not{p} \omega_+ \right) \left. \right] - m_t |m_3| e^{i\theta_3} (Z_t^\dagger)_{j,2} \\
& \times \left[\frac{4}{D} \frac{q_1^2}{q_1^2 - m_{\tilde{s}_i}^2} (2p+k)_\mu \omega_+ + \frac{4}{D} \frac{q_1 \cdot q_2}{q_2^2 - m_{H^+}^2} p_\mu \omega_+ - (2p+k)_\mu \omega_+ \right] \Big\}. \tag{13}
\end{aligned}$$

In a similar way, we can obtain the other triangle diagram amplitudes.

(iii) Using loop momentum translation invariance, we formulate the sum of those amplitudes in gauge invariant form explicitly, then extract the corresponding Wilson coefficients which are expressed by the two-loop vacuum integrals [14]. In fact, there are many identities among those two-loop integrations. In order to obtain those necessary identities which are used to simplify the sum of those triangle amplitudes, we start from the zero in-

tegration such as

$$\int \frac{d^D q_1}{(2\pi)^D} \frac{d^D q_2}{(2\pi)^D} \frac{q_1 \cdot p \not{q}_1 (\not{q}_2 - \not{q}_1)}{\mathcal{D}_0} \equiv 0. \tag{14}$$

Under the loop momentum translation $q_2 \rightarrow q_2 - a$, where a is same order as the external momentum p in magnitude, we expand the integration in powers of the momenta p, a to the second order

$$\begin{aligned}
\int \frac{d^D q_1}{(2\pi)^D} \frac{d^D q_2}{(2\pi)^D} \frac{q_1 \cdot p}{\mathcal{D}_0} \not{q}_1 (\not{q}_2 - \not{q}_1) &= \int \frac{d^D q_1}{(2\pi)^D} \frac{d^D q_2}{(2\pi)^D} \frac{q_1 \cdot p}{\mathcal{D}_0} \left\{ 1 + \frac{2(q_2 - q_1) \cdot a}{(q_2 - q_1)^2 - m_0^2} + \frac{2q_2 \cdot a}{q_2^2 - m_\alpha^2} \right\} \{ \not{q}_1 (\not{q}_2 - \not{q}_1) - \not{q}_1 \not{a} \} \\
&= \int \frac{d^D q_1}{(2\pi)^D} \frac{d^D q_2}{(2\pi)^D} \frac{1}{\mathcal{D}_0} \left\{ -\frac{q_1^2}{D} \not{p} \not{a} + \frac{2}{(q_2 - q_1)^2 - m_0^2} \right. \\
&\quad \times \left[\left(\frac{D(q_1 \cdot q_2)^2 - q_1^2 q_2^2}{D(D-1)} + \frac{q_1^4 - 2q_1^2 q_1 \cdot q_2}{D} \right) (p \cdot a) - \frac{(q_1 \cdot q_2)^2 - q_1^2 q_2^2}{D(D-1)} (\not{p} \not{a}) \right] \\
&\quad \left. + \frac{2}{q_2^2 - m_\alpha^2} \left[\left(\frac{D(q_1 \cdot q_2)^2 - q_1^2 q_2^2}{D(D-1)} - \frac{q_1^2 q_1 \cdot q_2}{D} \right) (p \cdot a) - \frac{(q_1 \cdot q_2)^2 - q_1^2 q_2^2}{D(D-1)} (\not{p} \not{a}) \right] \right\} \\
&\equiv 0. \tag{15}
\end{aligned}$$

The above identical equation implies

$$\begin{aligned}
&\int \frac{d^D q_1}{(2\pi)^D} \frac{d^D q_2}{(2\pi)^D} \frac{1}{\mathcal{D}_0} \left\{ \frac{1}{(q_2 - q_1)^2 - m_0^2} \left[\frac{D(q_1 \cdot q_2)^2 - q_1^2 q_2^2}{D(D-1)} + \frac{q_1^4 - 2q_1^2 q_1 \cdot q_2}{D} \right] + \right. \\
&\quad \left. \frac{1}{q_2^2 - m_\alpha^2} \left[\frac{D(q_1 \cdot q_2)^2 - q_1^2 q_2^2}{D(D-1)} - \frac{q_1^2 q_1 \cdot q_2}{D} \right] \right\} \equiv 0, \tag{16} \\
&\int \frac{d^D q_1}{(2\pi)^D} \frac{d^D q_2}{(2\pi)^D} \frac{1}{\mathcal{D}_0} \left\{ \frac{2}{(q_2 - q_1)^2 - m_0^2} \frac{(q_1 \cdot q_2)^2 - q_1^2 q_2^2}{D(D-1)} + \frac{2}{q_2^2 - m_\alpha^2} \frac{(q_1 \cdot q_2)^2 - q_1^2 q_2^2}{D(D-1)} + \frac{q_1^2}{D} \right\} \equiv 0.
\end{aligned}$$

Similarly, we can get the following identities from the invariance of Eq. (14) under the loop momentum translation $q_1 \rightarrow q_1 - a, q_2 \rightarrow q_2 - a$:

$$\begin{aligned}
&\int \frac{d^D q_1}{(2\pi)^D} \frac{d^D q_2}{(2\pi)^D} \frac{1}{\mathcal{D}_0} \left\{ -\frac{2+D}{D} q_1 \cdot (q_2 - q_1) + \frac{2}{q_1^2 - m_\alpha^2} \frac{q_1^2 q_1 \cdot (q_2 - q_1)}{D} + \right. \\
&\quad \left. \frac{2}{q_2^2 - m_\alpha^2} \left[\frac{D(q_1 \cdot q_2)^2 - q_1^2 q_2^2}{D(D-1)} - \frac{q_1^2 q_1 \cdot q_2}{D} \right] \right\} \equiv 0, \tag{17} \\
&\int \frac{d^D q_1}{(2\pi)^D} \frac{d^D q_2}{(2\pi)^D} \frac{1}{\mathcal{D}_0} \left\{ \frac{q_1 \cdot (q_2 - q_1)}{D} - \frac{2}{q_2^2 - m_\alpha^2} \frac{(q_1 \cdot q_2)^2 - q_1^2 q_2^2}{D(D-1)} \right\} \equiv 0.
\end{aligned}$$

Using the concrete expressions of two-loop vacuum integrals in Ref. [14], we can also verify those equations in Eqs. (16) and (17) directly after some tedious calculations. Replacing the numerator of Eq. (14) with other odd rank tensors in loop momenta, the more additional identities among two-loop integrations are gotten. In general, those identities are linearly dependent. After some simplification, we obtain those linearly independent equations in Appendix A. Certainly, those linearly inde-

pendent equations can also be derived from the two-loop integrations in which numerators are even rank tensors of loop momenta. However, the process to derive the linearly independent equations with the numerators in even powers of loop momenta is more complicated than that with the numerators in odd powers of loop momenta.

After the above procedure, we finally obtain the relevant coefficients from the charged Higgs contribution up to $\mathcal{O}(\alpha_s \tan\beta)$

$$\begin{aligned} C_{7,H}(\mu_w) &= \frac{8\sqrt{2}}{3} (4\pi)^3 e_d(\alpha_s \tan\beta) (Z_{\bar{s}})_{2,i} (Z_s^\dagger)_{i,2} \left[|\mu| m_t e^{-i\theta_\mu} (Z_{\bar{t}})_{2,j} + \frac{\sqrt{2} s_w m_w A_s}{e} (Z_{\bar{t}})_{1,j} \right] \\ &\quad \times \int \frac{d^4 q_1}{(2\pi)^4} \frac{d^4 q_2}{(2\pi)^4} \frac{1}{\mathcal{D}_H} \left\{ (Z_{\bar{t}}^\dagger)_{j,1} \mathcal{N}_{H(1)}^\gamma - m_t |m_3| e^{i\theta_3} (Z_{\bar{t}}^\dagger)_{j,2} \mathcal{N}_{H(2)}^\gamma \right\}, \\ C_{8,H}(\mu_w) &= \frac{8\sqrt{2}}{3} (4\pi)^3 (\alpha_s \tan\beta) (Z_{\bar{s}})_{2,i} (Z_s^\dagger)_{i,2} \left[|\mu| m_t e^{-i\theta_\mu} (Z_{\bar{t}})_{2,j} + \frac{\sqrt{2} s_w m_w A_s}{e} (Z_{\bar{t}})_{1,j} \right] \\ &\quad \times \int \frac{d^4 q_1}{(2\pi)^4} \frac{d^4 q_2}{(2\pi)^4} \frac{1}{\mathcal{D}_H} \left\{ (Z_{\bar{t}}^\dagger)_{j,1} \mathcal{N}_{H(1)}^g - m_t |m_3| e^{i\theta_3} (Z_{\bar{t}}^\dagger)_{j,2} \mathcal{N}_{H(2)}^g \right\}, \end{aligned} \quad (18)$$

where $\alpha_s = g_s^2/4\pi$, and the expressions of the form factors $\mathcal{N}_{H(1,2)}^{\gamma,g}$ can be found in Appendix B. Note, Ref. [10] has also obtained the Wilson coefficients from the same diagrams. We formulate our expressions in the more concise forms using the identities from Appendix A. For the chargino contribution that is ignored by Ref. [10], we can similarly have

$$\begin{aligned} C_{7,\chi_k}(\mu_w) &= \frac{8\sqrt{2}}{3} e_d (4\pi)^3 (\alpha_s \tan\beta) (Z_{\bar{s}})_{2,i} (Z_s^\dagger)_{i,2} (Z_{\bar{t}}^\dagger)_{j,1} (Z_{\bar{t}}^\dagger)_{k,2} \int \frac{d^4 q_1}{(2\pi)^4} \frac{d^4 q_2}{(2\pi)^4} \frac{1}{\mathcal{D}_{\chi_k}} \\ &\quad \times \left\{ m_t m_{\chi_k} (Z_{\bar{t}})_{2,j} (Z_+)_{2,k} \mathcal{N}_{\chi_k^\pm(1)}^\gamma + \sqrt{2} m_w m_t (Z_{\bar{t}})_{2,j} (Z_-)_{1,k} \mathcal{N}_{\chi_k^\pm(2)}^\gamma - \sqrt{2} m_w |m_3| e^{i\theta_3} (Z_{\bar{t}})_{1,j} (Z_-)_{1,k} \mathcal{N}_{\chi_k^\pm(3)}^\gamma \right. \\ &\quad \left. + m_{\bar{t}}^2 m_{\chi_k} |m_3| e^{i\theta_3} (Z_{\bar{t}})_{1,j} (Z_+)_{2,k} \mathcal{N}_{\chi_k^\pm(4)}^\gamma \right\}, \\ C_{8,\chi_k}(\mu_w) &= \frac{8\sqrt{2}}{3} (4\pi)^3 (\alpha_s \tan\beta) (Z_{\bar{s}})_{2,i} (Z_s^\dagger)_{i,2} (Z_{\bar{t}}^\dagger)_{j,1} (Z_{\bar{t}}^\dagger)_{k,2} \int \frac{d^4 q_1}{(2\pi)^4} \frac{d^4 q_2}{(2\pi)^4} \frac{1}{\mathcal{D}_{\chi_k}} \\ &\quad \times \left\{ m_t m_{\chi_k} (Z_{\bar{t}})_{2,j} (Z_+)_{2,k} \mathcal{N}_{\chi_k^\pm(1)}^g + \sqrt{2} m_w m_t (Z_{\bar{t}})_{2,j} (Z_-)_{1,k} \mathcal{N}_{\chi_k^\pm(2)}^g \right. \\ &\quad \left. - \sqrt{2} m_w |m_3| e^{i\theta_3} (Z_{\bar{t}})_{1,j} (Z_-)_{1,k} \mathcal{N}_{\chi_k^\pm(3)}^g + m_{\bar{t}}^2 m_{\chi_k} |m_3| e^{i\theta_3} (Z_{\bar{t}})_{1,j} (Z_+)_{2,k} \mathcal{N}_{\chi_k^\pm(4)}^g \right\}, \end{aligned} \quad (19)$$

with $\mathcal{D}_{\chi_k} = [(q_2 - q_1)^2 - m_{\bar{t}}^2](q_1^2 - |m_3|^2)(q_1^2 - m_{\bar{s}}^2) \times (q_2^2 - m_{\bar{t}}^2)(q_2^2 - m_{\chi_k}^2)$. Z_- , Z_+ are the left- and right-handed mixing matrices of charginos, and the form factors $\mathcal{N}_{\chi_k^\pm(i)}^{\gamma,g}$ ($i = 1, 2, 3, 4$) are collected in Appendix B. After we simplify the sum of the $\bar{s}b\gamma(g)$ triangle diagram amplitudes using the identities in Appendix A, we find that the effective $\bar{s}b\gamma(g)$ vertices should also include the two-point operator

$$\mathcal{O}_{\text{se}} = \frac{1}{(4\pi)^2} m_b(\mu) \bar{s}_L (i\not{D})^2 b_R, \quad (20)$$

beside the magnetic (chromomagnetic) dipole operators \mathcal{O}_7 (\mathcal{O}_8). Here, the covariant derivative acting on the quark fields is

$$D_\mu = \partial_\mu - i e e_q A_\mu - i g_s G_\mu, \quad (21)$$

with $G_\mu = G_\mu^a T^a$. Certainly, the Wilson coefficient of this operator does not give any contribution to the rare process $b \rightarrow s\gamma$ after we evolve the corresponding coefficients from the matching EW scale to the hadronic scale. Nevertheless, when we extract the Wilson coefficients of \mathcal{O}_7 (\mathcal{O}_8), it makes sense to keep this operator for the following reason. Beside the effective vertex with two quarks

$$\mathcal{O}_{\text{se}} \sim \frac{i}{(4\pi)^2} m_b p^2 \omega_+, \quad (22)$$

the operator \mathcal{O}_{se} can also induce the effective vertices with two quarks and one photon or gluon

$$\begin{aligned} \mathcal{O}_{se} &\sim \frac{i}{(4\pi)^2} ee_d m_b (2p_\mu + \not{k} \gamma_\mu) \omega_+, \\ \mathcal{O}_{se} &\sim \frac{i}{(4\pi)^2} g_s T^a m_b (2p_\mu + \not{k} \gamma_\mu) \omega_+ \end{aligned} \quad (23)$$

in the momentum space. Here, p, k are the incoming momenta of the external quark b and gauge boson (γ or g), respectively. For the effective $\bar{s}b\gamma(g)$ vertices $A_\mu^{\gamma(g)}(p, k)$, the corresponding WTIs required by the $SU(3)_c \times U(1)_{em}$ gauge invariance are written as

$$\begin{aligned} iee_d[\Sigma(p+k) - \Sigma(p)] &= ik \cdot A^\gamma(p, k), \\ ig_s T^a[\Sigma(p+k) - \Sigma(p)] &= ik \cdot A^g(p, k), \end{aligned} \quad (24)$$

where $i\Sigma(p)$ represents the sum of amplitudes for the self-energy diagrams (Fig. 1). Expanding the self-energy amplitudes in powers of external momentum to the third order, we have

$$i\Sigma(p) = \frac{i}{(4\pi)^2} B_0 m_b p^2, \quad (25)$$

where the function B_0 only depends on the heavy freedoms which are integrated out. In the effective theory, there are two deductions from the WTIs:

(i) the effective $\bar{s}b\gamma(g)$ vertices can be formulated as

$$\begin{aligned} iA_\mu^\gamma(p, k) &= \frac{i}{(4\pi)^2} ee_d m_b \{B_1^\gamma(2p_\mu + \not{k} \gamma_\mu) \\ &\quad + B_2^\gamma[\not{k}, \gamma_\mu]\} \omega_+, \\ iA_\mu^g(p, k) &= \frac{i}{(4\pi)^2} g_s T^a m_b \{B_1^g(2p_\mu + \not{k} \gamma_\mu) \\ &\quad + B_2^g[\not{k}, \gamma_\mu]\} \omega_+ \end{aligned} \quad (26)$$

after we expand $A_\mu^{\gamma(g)}(p, k)$ in powers of external momenta to the second order, where $B_{1,2}^{\gamma,g}$ are the functions of heavy freedoms only;

(ii) additionally, $B_0 = B_1^\gamma = B_1^g$. The above deductions can be taken as the criterion to test our calculations. In Eq. (26), the functions $B_2^{\gamma,g}$ are proportional to the Wilson coefficients of the magnetic and chromomagnetic dipole operators, respectively.

As an application, we will investigate the CP asymmetry of the rare decay $B \rightarrow X_s \gamma$ within the framework of MSSM.

III. DIRECT CP VIOLATION IN $B \rightarrow X_s \gamma$

In the SM, the CP asymmetry of the $B \rightarrow X_s \gamma$ process

$$A_{CP}(B \rightarrow X_s \gamma) = \frac{\Gamma(\bar{B} \rightarrow X_s \gamma) - \Gamma(B \rightarrow X_s \gamma)}{\Gamma(\bar{B} \rightarrow X_s \gamma) + \Gamma(B \rightarrow X_s \gamma)} \quad (27)$$

is calculated to be rather small: $A_{CP} \sim 0.5\%$ [15]. For

experimental data, the recent measurement [16] of the CP asymmetry implies the 95% range of

$$-0.30 \leq A_{CP}(B \rightarrow X_s \gamma) \leq 0.14. \quad (28)$$

In other words, studies of the direct CP asymmetry in $B \rightarrow X_s \gamma$ may uncover new sources of the CP violation which lie outside the SM. Up to the NLO, the complete theoretical prediction has been presented in Ref. [17]. In order to eliminate the strong dependence on the b -quark mass, the branching ratios is usually normalized by the decay rate of the B meson semileptonic decay:

$$\frac{\Gamma(B \rightarrow X_s \gamma)}{\Gamma(B \rightarrow X_c e \bar{\nu})} = \frac{6\alpha}{\pi f(z)} \left| \frac{V_{ts}^* V_{tb}}{V_{cb}} C_7(\mu_b) \right|^2, \quad (29)$$

where $f(z) = 1 - 8z + 8z^3 - z^4 - 12z^2 \ln z$ is the phase-space factor with $z = (m_c/m_b)^2$, and $\alpha = e^2/(4\pi)$ is the EW fine-structure constant. The CP asymmetry in the rare decay $B \rightarrow X_s \gamma$ is correspondingly formulated as [15]

$$\begin{aligned} A_{CP}(B \rightarrow X_s \gamma) &= \frac{\alpha_s(\mu_b)}{|C_7(\mu_b)|^2} \left\{ \frac{40}{81} \text{Im}[C_2(\mu_b) C_7^*(\mu_b)] \right. \\ &\quad - \frac{4}{9} \text{Im}[C_8(\mu_b) C_7^*(\mu_b)] - \frac{8z}{9} g(z) \text{Im} \\ &\quad \times \left[\left(1 + \frac{V_{us}^* V_{ub}}{V_{ts}^* V_{tb}} \right) C_2(\mu_b) C_7^*(\mu_b) \right] \left. \right\}, \end{aligned} \quad (30)$$

with $g(z) = (5 + \ln z + \ln^2 z - \pi^2/3) + (\ln^2 z - \pi^2/3)z + (28/9 - 4/3 \ln z)z^2 + \mathcal{O}(z^3)$. The $C_2(\mu_b)$ is the Wilson coefficient of the operator $\mathcal{O}_2 = \bar{s}_L \gamma_\mu q_L \bar{q}_L \gamma^\mu b_L$ ($q = c, u$) at the hadronic scale. From now on we shall assume the value $BR(B \rightarrow X_c e \bar{\nu}) = 10.5\%$ for the semileptonic branching ratio, $\alpha_s(m_z) = 0.118$, $\alpha(m_z) = 1/127$. For the standard particle masses, we take $m_t = 174$, $m_b = 4.2$, $m_w = 80.42$, $m_z = 91.19$ GeV, and $z = m_c/m_b = 0.29$. In the CKM matrix, we apply the Wolfenstein parametrization and set $A = 0.85$, $\lambda = 0.22$, $\rho = 0.22$, $\eta = 0.35$ [18]. Without loss of generality, we always assume the supersymmetric parameters $\mu = A_t e^{-i\pi/2} = 100$, $m_3 e^{-i\pi/4} = 300$, $A_s e^{-i\pi/2} = m_{t_R} = 200$ GeV, $m_{t_L} = m_{s_L} = 5$ TeV here. In order to suppress the one-loop EDMs, we choose the μ parameter CP phase $\theta_\mu = 0$. As for the CP phase which is contained in the $SU(2)$ gaugino mass parameter m_2 , it is set as $\theta_2 = \arg(m_2) = \pi/4$.

Taking $\tan\beta = 30$, $|m_2| = 300$ GeV, $m_{s_R} = 500$ GeV, we plot the CP asymmetry and branching ratio of the inclusive $B \rightarrow X_s \gamma$ decay versus the charged Higgs mass in Fig. 4. Considering the experimental constraint on the

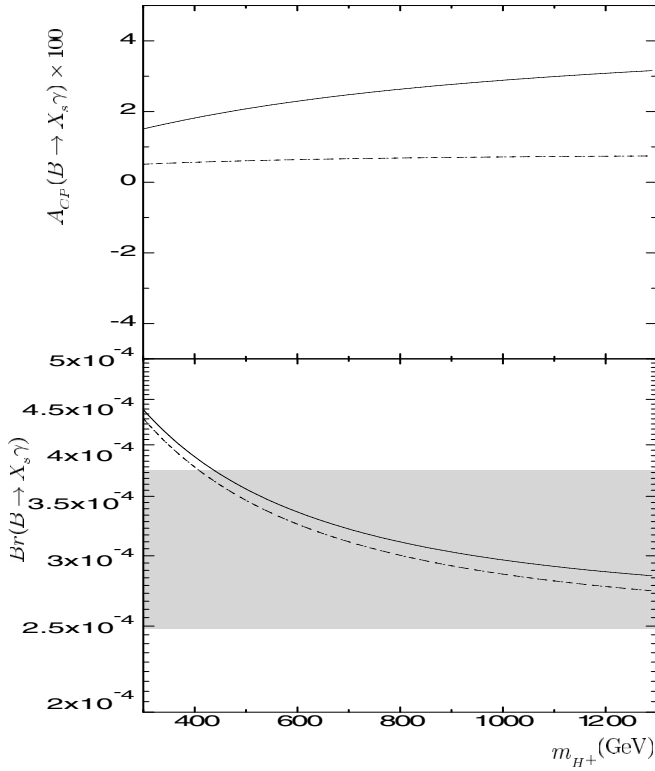


FIG. 4. The CP asymmetry and branching ratio of the inclusive $B \rightarrow X_s \gamma$ decay versus the charged Higgs mass m_{H^+} . Dashed line: theoretical prediction at the one-loop order; solid line: theoretical prediction at the two-loop order, when $\tan\beta = 30$, $|m_2| = 300$ GeV, $m_{s_R} = 500$ GeV, the other parameters are taken as in the text. The gray band is the experimental allowed region for the branching ratio $BR(B \rightarrow X_s \gamma)$ at 1σ deviation.

branching ratio $BR(B \rightarrow X_s \gamma)$ at 1σ tolerance, the CP asymmetry including the two-loop corrections can be larger than 3%, and the one-loop result is smaller than 1% with our chosen parameters. The choice of parameter space of Fig. 5 is identical with that of Fig. 4 except for $\tan\beta = 60$. After including the two-loop corrections, we find that the CP asymmetry can reach 5% with an increasing of the charged Higgs mass when $\tan\beta = 60$, while at the same time keeping the branching ratio $BR(B \rightarrow X_s \gamma)$ within the 1σ deviation experimental bound. Since the two-loop correction is proportional to $\tan\beta$, we can understand why the differences between the one- and two-loop predictions of Fig. 5 ($\tan\beta = 60$) are larger than that of Fig. 4 ($\tan\beta = 30$). From the numerical analysis, we find that the two-loop corrections to the Wilson coefficients are still rather smaller than the one-loop results at $\tan\beta = 30$, while the two-loop corrections are comparable with the one-loop results at $\tan\beta = 60$. Since the bottom quark Yukawa coupling approximates to 1 at $\tan\beta = 60$, it should be argued whether or not we can safely apply the perturbative expansion to give the

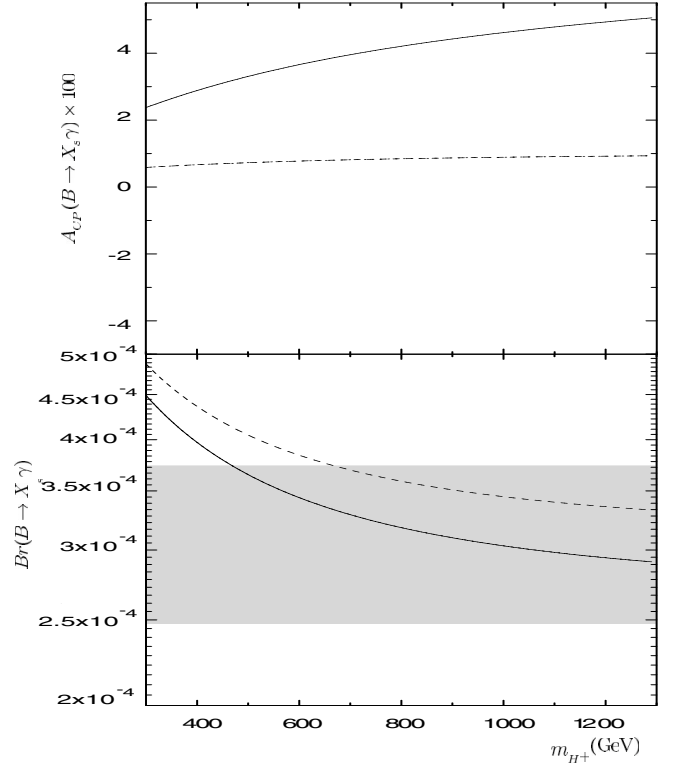


FIG. 5. The CP asymmetry and branching ratio of the inclusive $B \rightarrow X_s \gamma$ decay versus the charged Higgs mass m_{H^+} . Dashed line: theoretical prediction at the one-loop order; solid line: theoretical prediction at the two-loop order, when $\tan\beta = 60$, $|m_2| = 300$ GeV, $m_{s_R} = 500$ GeV, the other parameters are taken as in the text. The gray band is the experimental allowed region for the branching ratio $BR(B \rightarrow X_s \gamma)$ at 1σ deviation.

theoretical predictions of physics observables for such high $\tan\beta$.

Now, let us study the variance of two-loop results with the soft $SU(2)$ gaugino mass parameter $|m_2|$. Taking $\tan\beta = 30$, $m_{s_R} = 200$ GeV, $m_{H^+} = 600$ GeV, we plot the theoretical predictions for the CP asymmetry and branching ratio of the inclusive $B \rightarrow X_s \gamma$ decay versus the parameter $|m_2|$ in Fig. 6 at one- and two-loop order, respectively. If the theoretical prediction for the branching ratio satisfies with the experimental bound at 1σ deviation

$$2.48 \times 10^{-4} \leq BR(B \rightarrow X_s \gamma) \leq 3.74 \times 10^{-4},$$

the CP asymmetry including the two-loop corrections is about $\sim 1.5\%$. The choice of the parameter space in Fig. 7 is identical with that of Fig. 6 except for $\tan\beta = 60$. In this scenario, the two-loop prediction on the asymmetry is about $\sim 4\%$. Note that the dependence of the two-loop corrections on the parameter $|m_2|$ is milder than that on the charged Higgs mass m_{H^+} . This fact can be understood as follows: the amplitudes of the correspond-

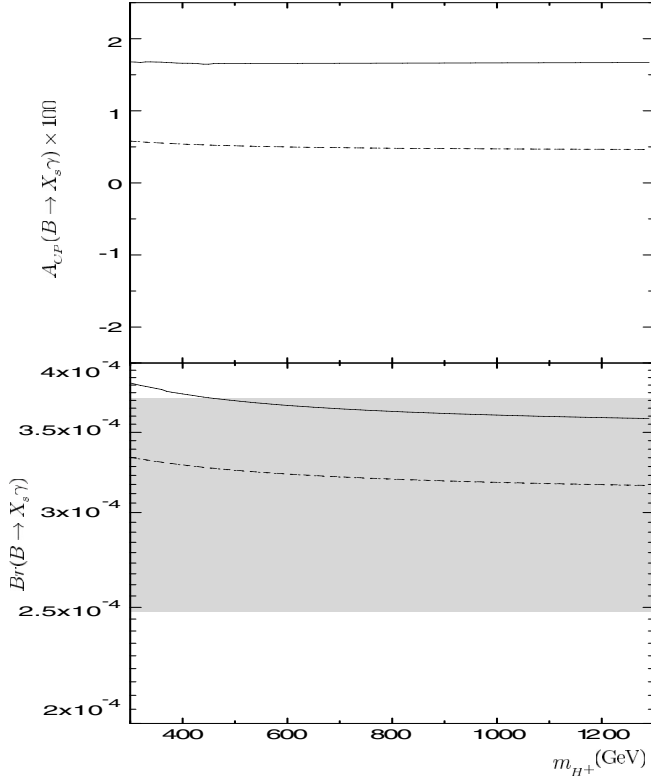


FIG. 6. The CP asymmetry and branching ratio of the inclusive $B \rightarrow X_s \gamma$ decay versus the parameter $|m_2|$. Dashed line: theoretical prediction at the one-loop order; solid line: theoretical prediction at the two-loop order, when $\tan\beta = 30$, $m_{H^+} = 600$ GeV, $m_{s_R} = 200$ GeV, the other parameters are taken as in the text. The gray band is the experimental allowed region for the branching ratio $BR(B \rightarrow X_s \gamma)$ at 1σ deviation.

ing triangle diagrams depend on the charged Higgs mass in the form $1/(Q^2 - m_{H^+}^2)$ (Q denotes loop momenta q_1, q_2 , or $q_2 - q_1$), and depend on the parameter $|m_2|$ through the chargino propagator $(\not{Q} - m_\chi)/(Q^2 - m_\chi^2)$ (m_χ denotes the chargino mass) before the loop momentum integration.

In our analysis, we do not compare the exact two-loop analysis with the HME result since the discussion has already been presented in Ref. [10].

IV. CONCLUSIONS

In this work, we present the complete two-loop gluino corrections to inclusive $B \rightarrow X_s \gamma$ decay in explicit CP violating MSSM within large $\tan\beta$ scenarios. Beside the diagrams where quark flavor change is mediated by the charged Higgs, we also include those diagrams in which quark flavor change is mediated by the charginos. Using loop momentum translation invariance, we formulate our

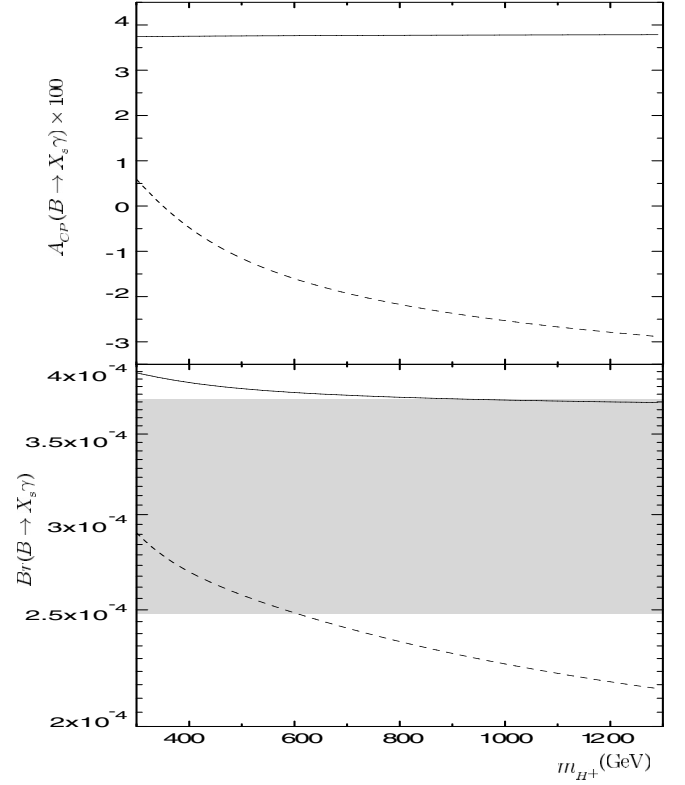


FIG. 7. The CP asymmetry and branching ratio of the inclusive $B \rightarrow X_s \gamma$ decay versus the parameter $|m_2|$. Dashed line: theoretical prediction at the one-loop order; solid line: theoretical prediction at the two-loop order, when $\tan\beta = 60$, $m_{H^+} = 600$ GeV, $m_{s_R} = 200$ GeV, the other parameters are taken as in the text. The gray band is the experimental allowed region for the branching ratio $BR(B \rightarrow X_s \gamma)$ at 1σ deviation.

expressions fulfilling the $SU(3)_c \times U(1)_{em}$ WTIs. From the numerical analysis, we show that the two-loop corrections to the branching ratio are comparable with the one-loop predictions at large $\tan\beta$. Correspondingly, the CP asymmetry can also reach about 5%, which is much larger than that predicted by the SM.

ACKNOWLEDGMENTS

The work has been supported by the Academy of Finland under Contracts No. 104915 and No. 107293.

APPENDIX A: IDENTITIES AMONG THE TWO-LOOP SCALAR INTEGRALS

Here, we report the identities that are used in the process of obtaining Eqs. (18) and (19). They can be derived from the loop momentum translation invariance of the amplitudes. They are

$$\begin{aligned}
& \int \frac{d^D q_1}{(2\pi)^D} \frac{d^D q_2}{(2\pi)^D} \frac{1}{\mathcal{D}_0} \left\{ \frac{q_1^2 q_1 \cdot (q_2 - q_1)}{(q_2 - q_1)^2 - m_0^2} + \frac{q_1^2 q_1 \cdot q_2}{q_2^2 - m_\alpha^2} \right\} \equiv 0, \\
& \int \frac{d^D q_1}{(2\pi)^D} \frac{d^D q_2}{(2\pi)^D} \frac{1}{\mathcal{D}_0} \left\{ \frac{2}{(q_2 - q_1)^2 - m_0^2} \frac{(q_1 \cdot q_2)^2 - q_1^2 q_2^2}{D(D-1)} + \frac{q_1 \cdot q_2}{D} \right\} \equiv 0, \\
& \int \frac{d^D q_1}{(2\pi)^D} \frac{d^D q_2}{(2\pi)^D} \frac{1}{\mathcal{D}_0} \left\{ -\frac{q_1 \cdot (q_2 - q_1)}{D} + \frac{2}{q_2^2 - m_\alpha^2} \frac{(q_1 \cdot q_2)^2 - q_1^2 q_2^2}{D(D-1)} \right\} \equiv 0, \\
& \int \frac{d^D q_1}{(2\pi)^D} \frac{d^D q_2}{(2\pi)^D} \frac{1}{\mathcal{D}_0} \left\{ \frac{1}{(q_2 - q_1)^2 - m_0^2} \left[\frac{D(q_1 \cdot q_2)^2 - q_1^2 q_2^2}{D(D-1)} - \frac{q_1^2 q_1 \cdot q_2}{D} \right] + \frac{1}{q_2^2 - m_\alpha^2} \frac{D(q_1 \cdot q_2)^2 - q_1^2 q_2^2}{D(D-1)} \right\} \equiv 0, \\
& \int \frac{d^D q_1}{(2\pi)^D} \frac{d^D q_2}{(2\pi)^D} \frac{1}{\mathcal{D}_0} \left\{ -q_1^2 + \frac{2}{D} \frac{q_1^2 q_2 \cdot (q_2 - q_1)}{(q_2 - q_1)^2 - m_0^2} + \frac{2}{D} \frac{q_1^2 q_2^2}{q_2^2 - m_\alpha^2} \right\} \equiv 0, \\
& \int \frac{d^D q_1}{(2\pi)^D} \frac{d^D q_2}{(2\pi)^D} \frac{1}{\mathcal{D}_0} \left\{ -\frac{2+D}{2} q_2^2 + \frac{q_2^2 q_2 \cdot (q_2 - q_1)}{(q_2 - q_1)^2 - m_0^2} + \frac{q_2^4}{q_2^2 - m_\alpha^2} \right\} \equiv 0, \\
& \int \frac{d^D q_1}{(2\pi)^D} \frac{d^D q_2}{(2\pi)^D} \frac{1}{\mathcal{D}_0} \left\{ -q_1 \cdot q_2 + \frac{2}{(q_2 - q_1)^2 - m_0^2} \frac{q_1 \cdot q_2 (q_2 - q_1)^2}{D} + \frac{2}{q_2^2 - m_\alpha^2} \left[\frac{q_1 \cdot q_2 q_2^2}{D} - \frac{D(q_1 \cdot q_2)^2 - q_1^2 q_2^2}{D(D-1)} \right] \right\} \equiv 0, \\
& \int \frac{d^D q_1}{(2\pi)^D} \frac{d^D q_2}{(2\pi)^D} \frac{1}{\mathcal{D}_0} \left\{ \frac{1}{(q_2 - q_1)^2 - m_0^2} \left[q_1 \cdot q_2 q_2 \cdot (q_2 - q_1) - \frac{D+1}{2} q_2^2 q_1 \cdot (q_2 - q_1) \right] - \frac{D-1}{2} \frac{q_2^2 q_1 \cdot q_2}{q_2^2 - m_\alpha^2} \right\} \equiv 0, \\
& \int \frac{d^D q_1}{(2\pi)^D} \frac{d^D q_2}{(2\pi)^D} \frac{1}{\mathcal{D}_0} \left\{ \frac{2}{D} \frac{q_2 \cdot (q_2 - q_1)}{(q_2 - q_1)^2 - m_0^2} + \frac{2}{D} \frac{q_2^2}{q_2^2 - m_\alpha^2} - 1 \right\} \equiv 0, \\
& \int \frac{d^D q_1}{(2\pi)^D} \frac{d^D q_2}{(2\pi)^D} \frac{1}{\mathcal{D}_0} \left\{ \frac{2}{D} \frac{(q_2 - q_1)^2}{(q_2 - q_1)^2 - m_0^2} + \frac{2}{D} \frac{q_2 \cdot (q_2 - q_1)}{q_2^2 - m_\alpha^2} - 1 \right\} \equiv 0, \\
& \int \frac{d^D q_1}{(2\pi)^D} \frac{d^D q_2}{(2\pi)^D} \frac{1}{\mathcal{D}_0} \left\{ \frac{q_1 \cdot (q_2 - q_1)}{D} - \frac{2}{q_2^2 - m_\alpha^2} \frac{(q_1 \cdot q_2)^2 - q_1^2 q_2^2}{D(D-1)} \right\} \equiv 0, \\
& \int \frac{d^D q_1}{(2\pi)^D} \frac{d^D q_2}{(2\pi)^D} \frac{1}{\mathcal{D}_0} \left\{ \frac{q_2 \cdot (q_2 - q_1)}{D} + \frac{2}{q_1^2 - m_a^2} \frac{(q_1 \cdot q_2)^2 - q_1^2 q_2^2}{D(D-1)} \right\} \equiv 0, \\
& \int \frac{d^D q_1}{(2\pi)^D} \frac{d^D q_2}{(2\pi)^D} \frac{1}{\mathcal{D}_0} \left\{ -\frac{2+D}{D} q_1 \cdot q_2 + \frac{2}{q_1^2 - m_a^2} \frac{q_1^2 q_1 \cdot q_2}{D} + \frac{2}{q_2^2 - m_\alpha^2} \frac{D(q_1 \cdot q_2)^2 - q_1^2 q_2^2}{D(D-1)} \right\} \equiv 0, \\
& \int \frac{d^D q_1}{(2\pi)^D} \frac{d^D q_2}{(2\pi)^D} \frac{1}{\mathcal{D}_0} \left\{ -\frac{2+D}{D} q_1 \cdot q_2 + \frac{2}{q_1^2 - m_a^2} \frac{D(q_1 \cdot q_2)^2 - q_1^2 q_2^2}{D(D-1)} + \frac{2}{q_2^2 - m_\alpha^2} \frac{q_1 \cdot q_2 q_2^2}{D} \right\} \equiv 0, \\
& \int \frac{d^D q_1}{(2\pi)^D} \frac{d^D q_2}{(2\pi)^D} \frac{1}{\mathcal{D}_0} \left\{ -\frac{2+D}{2} q_1^2 + \frac{q_1^4}{q_1^2 - m_a^2} + \frac{q_1^2 q_1 \cdot q_2}{q_2^2 - m_\alpha^2} \right\} \equiv 0, \\
& \int \frac{d^D q_1}{(2\pi)^D} \frac{d^D q_2}{(2\pi)^D} \frac{1}{\mathcal{D}_0} \left\{ -\frac{2+D}{2} q_2^2 + \frac{q_1 \cdot q_2 q_2^2}{q_1^2 - m_a^2} + \frac{q_2^4}{q_2^2 - m_\alpha^2} \right\} \equiv 0, \\
& \int \frac{d^D q_1}{(2\pi)^D} \frac{d^D q_2}{(2\pi)^D} \frac{1}{\mathcal{D}_0} \left\{ -q_2 \cdot (q_2 - q_1) + \frac{q_1 \cdot (q_2 - q_1) q_2^2}{q_1^2 - m_a^2} + \frac{q_2 \cdot (q_2 - q_1) q_2^2}{q_2^2 - m_\alpha^2} \right\} \equiv 0, \\
& \int \frac{d^D q_1}{(2\pi)^D} \frac{d^D q_2}{(2\pi)^D} \frac{1}{\mathcal{D}_0} \left\{ \frac{2}{D} \frac{q_1^2}{q_1^2 - m_a^2} + \frac{2}{D} \frac{q_1 \cdot q_2}{q_2^2 - m_\alpha^2} - 1 \right\} \equiv 0, \\
& \int \frac{d^D q_1}{(2\pi)^D} \frac{d^D q_2}{(2\pi)^D} \frac{1}{\mathcal{D}_0} \left\{ \frac{2}{D} \frac{q_1 \cdot q_2}{q_1^2 - m_a^2} + \frac{2}{D} \frac{q_2^2}{q_2^2 - m_\alpha^2} - 1 \right\} \equiv 0,
\end{aligned} \tag{A1}$$

with $\mathcal{D}_0 = [(q_2 - q_1)^2 - m_0^2](q_1^2 - m_a^2)(q_2^2 - m_\alpha^2)$, and D is the time-space dimension. In addition the two-loop vacuum integral

$$\int \frac{d^D q_1}{(2\pi)^D} \frac{d^D q_2}{(2\pi)^D} \frac{1}{\mathcal{D}_0}, \quad (\text{A2})$$

has been discussed in Ref. [14].

APPENDIX B: FORM FACTORS IN THE TWO-LOOP WILSON COEFFICIENTS

$$\begin{aligned}
\mathcal{N}_{H(1)}^\gamma &= -\frac{q_1^2 q_1 \cdot q_2}{(q_1^2 - m_{\tilde{s}_i}^2)^2} - \frac{1}{3} \frac{4(q_1 \cdot q_2)^2 - q_1^2 q_2^2}{(q_1^2 - m_{\tilde{s}_i}^2)(q_2^2 - m_{H^+}^2)} - \frac{q_1 \cdot q_2 q_2^2}{(q_2^2 - m_{H^+}^2)^2} + \frac{q_1 \cdot q_2}{q_1^2 - m_{\tilde{s}_i}^2} + \frac{q_1 \cdot q_2}{q_2^2 - m_t^2}, \\
\mathcal{N}_{H(2)}^\gamma &= -\frac{q_1^2}{(q_1^2 - m_{\tilde{s}_i}^2)^2} - \frac{q_1 \cdot q_2}{(q_1^2 - m_{\tilde{s}_i}^2)(q_2^2 - m_{H^+}^2)} - \frac{q_2^2}{(q_2^2 - m_{H^+}^2)^2} + \frac{1}{q_1^2 - m_{\tilde{s}_i}^2} + \frac{1}{q_2^2 - m_{H^+}^2} + \frac{2}{q_2^2 - m_t^2} \Big], \\
\mathcal{N}_{H(1)}^g &= -\frac{q_1^2 q_1 \cdot q_2}{(q_1^2 - m_{\tilde{s}_i}^2)^2} - \frac{1}{3} \frac{4(q_1 \cdot q_2)^2 - q_1^2 q_2^2}{(q_1^2 - m_{\tilde{s}_i}^2)(q_2^2 - m_{H^+}^2)} - \frac{q_1 \cdot q_2 q_2^2}{(q_2^2 - m_{H^+}^2)^2} + \frac{17}{8} \frac{q_1 \cdot q_2}{q_1^2 - m_{\tilde{s}_i}^2} - \frac{1}{16} \frac{8q_1 \cdot q_2 - 9q_2^2}{q_2^2 - m_t^2} \\
&\quad + \frac{3}{16} \frac{8q_1 \cdot q_2 + 3q_2^2}{q_2^2 - m_{H^+}^2} - \frac{9}{16}, \\
\mathcal{N}_{H(2)}^g &= -\frac{q_1^2}{(q_1^2 - m_{\tilde{s}_i}^2)^2} - \frac{q_1 \cdot q_2}{(q_1^2 - m_{\tilde{s}_i}^2)(q_2^2 - m_{H^+}^2)} - \frac{q_2^2}{(q_2^2 - m_{H^+}^2)^2} + \frac{1}{q_1^2 - m_{\tilde{s}_i}^2} + \frac{1}{q_2^2 - m_{H^+}^2} - \frac{1}{q_2^2 - m_t^2} - \frac{9}{8} \frac{1}{q_1^2 - |m_3|^2}, \\
\mathcal{N}_{\chi_k^\pm(1)}^\gamma &= \frac{q_1^2 q_1 \cdot (q_2 - q_1)}{(q_1^2 - m_{\tilde{s}_i}^2)^2} - \frac{1}{3} \frac{3q_1^2 q_1 \cdot q_2 - 4(q_1 \cdot q_2)^2 + q_1^2 q_2^2}{(q_1^2 - m_{\tilde{s}_i}^2)(q_2^2 - m_{\chi_k}^2)} + \frac{q_1 \cdot (q_2 - q_1) q_2^2}{(q_2^2 - m_{\chi_k}^2)^2} - \frac{q_1 \cdot (q_2 - q_1)}{q_2^2 - m_{\tilde{l}_j}^2} - \frac{2q_1^2 - q_1 \cdot q_2}{q_2^2 - m_{\chi_k}^2} \\
&\quad - \frac{q_1 \cdot q_2}{q_2^2 - m_{\tilde{l}_j}^2}, \\
\mathcal{N}_{\chi_k^\pm(2)}^\gamma &= \frac{q_1^2 q_1 \cdot q_2}{(q_1^2 - m_{\tilde{s}_i}^2)^2} - \frac{1}{3} \frac{4(q_1 \cdot q_2)^2 - q_1^2 q_2^2}{(q_1^2 - m_{\tilde{s}_i}^2)(q_2^2 - m_{\chi_k}^2)} + \frac{q_1 \cdot q_2 q_2^2}{(q_2^2 - m_{\chi_k}^2)^2} - \frac{q_1 \cdot q_2}{q_1^2 - m_{\tilde{s}_i}^2} - \frac{q_1 \cdot q_2}{q_2^2 - m_{\tilde{l}_j}^2}, \\
\mathcal{N}_{\chi_k^\pm(3)}^\gamma &= \frac{q_1^2 q_2 \cdot (q_2 - q_1)}{(q_1^2 - m_{\tilde{s}_i}^2)^2} + \frac{1}{3} \frac{3q_1 \cdot q_2 q_2^2 - 4(q_1 \cdot q_2)^2 + q_1^2 q_2^2}{(q_1^2 - m_{\tilde{s}_i}^2)(q_2^2 - m_{\chi_k}^2)} + \frac{q_2 \cdot (q_2 - q_1) q_2^2}{(q_2^2 - m_{\chi_k}^2)^2} - \frac{q_2 \cdot (q_2 - q_1)}{q_1^2 - m_{\tilde{s}_i}^2} - \frac{q_2^2}{q_2^2 - m_{\chi_k}^2} \\
&\quad - \frac{2q_2^2 - q_1 \cdot q_2}{q_2^2 - m_{\tilde{l}_j}^2} - 2, \\
\mathcal{N}_{\chi_k^\pm(4)}^\gamma &= -\frac{q_1^2}{(q_1^2 - m_{\tilde{s}_i}^2)^2} - \frac{q_2^2}{(q_2^2 - m_{\chi_k}^2)^2} - \frac{q_1 \cdot q_2}{(q_1^2 - m_{\tilde{s}_i}^2)(q_2^2 - m_{\chi_k}^2)} + \frac{1}{q_1^2 - m_{\tilde{s}_i}^2} - \frac{2}{q_2^2 - m_{\chi_k}^2} - \frac{2}{(q_2 - q_1)^2 - m_t^2}, \\
\mathcal{N}_{\chi_k^\pm(1)}^g &= \frac{q_1^2 q_1 \cdot (q_2 - q_1)}{(q_1^2 - m_{\tilde{s}_i}^2)^2} - \frac{1}{3} \frac{3q_1^2 q_1 \cdot q_2 - 4(q_1 \cdot q_2)^2 + q_1^2 q_2^2}{(q_1^2 - m_{\tilde{s}_i}^2)(q_2^2 - m_{\chi_k}^2)} + \frac{q_1 \cdot (q_2 - q_1) q_2^2}{(q_2^2 - m_{\chi_k}^2)^2} - \frac{17}{8} \frac{q_1 \cdot (q_2 - q_1)}{q_1^2 - m_{\tilde{s}_i}^2} \\
&\quad - \frac{1}{16} \frac{7q_1 \cdot q_2 - q_1^2 + 9q_2^2}{q_2^2 - m_{\chi_k}^2} - \frac{9}{16} \frac{q_2 \cdot (q_2 - q_1)}{q_2^2 - m_{\tilde{l}_j}^2}, \\
\mathcal{N}_{\chi_k^\pm(2)}^g &= \frac{q_1^2 q_1 \cdot q_2}{(q_1^2 - m_{\tilde{s}_i}^2)^2} + \frac{1}{3} \frac{4(q_1 \cdot q_2)^2 - q_1^2 q_2^2}{(q_1^2 - m_{\tilde{s}_i}^2)(q_2^2 - m_{\chi_k}^2)} + \frac{q_1 \cdot q_2 q_2^2}{(q_2^2 - m_{\chi_k}^2)^2} - \frac{17}{8} \frac{q_1 \cdot q_2}{q_1^2 - m_{\tilde{s}_i}^2} - \frac{3}{16} \frac{8q_1 \cdot q_2 + 3q_2^2}{q_2^2 - m_{\chi_k}^2} + \frac{1}{16} \frac{8q_1 \cdot q_2 - 9q_2^2}{q_2^2 - m_{\tilde{l}_j}^2} \\
&\quad + \frac{9}{8}, \\
\mathcal{N}_{\chi_k^\pm(3)}^g &= \frac{q_1^2 q_2 \cdot (q_2 - q_1)}{(q_1^2 - m_{\tilde{s}_i}^2)^2} + \frac{1}{3} \frac{3q_1 \cdot q_2 q_2^2 - 4(q_1 \cdot q_2)^2 + q_1^2 q_2^2}{(q_1^2 - m_{\tilde{s}_i}^2)(q_2^2 - m_{\chi_k}^2)} + \frac{q_2 \cdot (q_2 - q_1) q_2^2}{(q_2^2 - m_{\chi_k}^2)^2} - \frac{q_2 \cdot (q_2 - q_1)}{q_1^2 - m_{\tilde{s}_i}^2} \\
&\quad + \frac{1}{8} \frac{12q_1 \cdot q_2 - 13q_2^2}{q_2^2 - m_{\chi_k}^2} + \frac{1}{16} \frac{7q_2^2 - 8q_1 \cdot q_2}{q_2^2 - m_{\tilde{l}_j}^2} + \frac{9}{8} \frac{q_2 \cdot (q_2 - q_1)}{q_1^2 - |m_3|^2} + \frac{1}{8}, \\
\mathcal{N}_{\chi_k^\pm(4)}^g &= -\frac{q_1^2}{(q_1^2 - m_{\tilde{s}_i}^2)^2} - \frac{q_1 \cdot q_2}{(q_1^2 - m_{\tilde{s}_i}^2)(q_2^2 - m_{\chi_k}^2)} + \frac{q_2^2}{(q_2^2 - m_{\chi_k}^2)^2} + \frac{1}{q_1^2 - m_{\tilde{s}_i}^2} + \frac{1}{q_2^2 - m_{\chi_k}^2} - \frac{9}{8} \frac{1}{q_1^2 - |m_3|^2} \\
&\quad - \frac{1}{8} \frac{1}{(q_2 - q_1)^2 - m_t^2}.
\end{aligned} \quad (\text{B1})$$

- [1] BELLE Collaboration, K. Abe *et al.*, Phys. Lett. B **511**, 151 (2001); CLEO Collaboration, S. Chen *et al.*, Phys. Rev. Lett. **87**, 251807 (2001); BABAR Collaboration, B. Aubert *et al.*, hep-ex/0207074; hep-ex/0207076.
- [2] K. Chetyrkin, M. Misiak, and M. Munz, Phys. Lett. B **400**, 206 (1997); **425**, 414(E) (1997); T. Hurth, hep-ph/0106050; C. Greub, T. Hurth, and D. Wyler, Phys. Rev. D **54**, 3350 (1996); K. Adel and Y. Yao, *ibid.* **49**, 4945 (1994); A. Ali and C. Greub, Phys. Lett. B **361**, 146 (1995).
- [3] A. Pilaftsis, Phys. Lett. B **435**, 88 (1998); D. A. Demir, Phys. Rev. D **60**, 055006 (1999); A. Pilaftsis and C. E. Wagner, Nucl. Phys. **B553**, 3 (1999); T. Ibrahim and P. Nath, Phys. Rev. D **63**, 035009 (2001); M. Carena, J. Ellis, A. Pilaftsis, and C. E. Wagner, Nucl. Phys. **B586**, 92 (2000); Phys. Lett. B **495**, 155 (2000).
- [4] T. Ibrahim and P. Nath, Phys. Lett. B **418**, 98 (1998); Phys. Rev. D **57**, 478 (1998); **58**, 111301 (1998); **61**, 093004 (2000); M. Brhlik, G. J. Good, and G. L. Kane, *ibid.* **59**, 115004 (1999); A. Bartl, T. Gajdosik, W. Porod, P. Stockinger, and H. Stremnitzer, *ibid.* **60**, 073003 (1999).
- [5] P. Nath, Phys. Rev. Lett. **66**, 2565 (1991); Y. Kizukuri and N. Oshimo, Phys. Rev. D **45**, 1806 (1992); **46**, 3025 (1992); D. Chang, W. Keung, and A. Pilaftsis, Phys. Rev. Lett. **82**, 900 (1999); A. Pilaftsis, Phys. Lett. B **471**, 174 (1999); D. Chang, W. Chang, and W. Keung, *ibid.* **478**, 239 (2000); T. F. Feng, T. Huang, X. Q. Li, X. M. Zhang, and S. M. Zhao, Phys. Rev. D **68**, 016004 (2003).
- [6] F. Kruger and J. C. Romao, Phys. Rev. D **62**, 034020 (2000); T. M. Aliev, D. A. Demir, and M. Savci, *ibid.* **62**, 074016 (2000).
- [7] D. A. Demir and M. B. Voloshin, Phys. Rev. D **63**, 115011 (2001).
- [8] A. Ali, H. Asatrian, and C. Greub, Phys. Lett. B **429**, 87 (1998); A. Ali and E. Lunghi, Eur. Phys. J. C **21**, 683 (2001); T. Nihei, Prog. Theor. Phys. **98**, 1157 (1997); S. Baek and P. Ko, Phys. Rev. Lett. **83**, 488 (1999); D. A. Demir, A. Masiero, and O. Vives, *ibid.* **82**, 2447 (1999); S. Baek, Phys. Rev. D **67**, 096004 (2003); A. Dedes and A. Pilaftsis, *ibid.* **67**, 015012 (2003).
- [9] H. Georgi, in *Particles and Fields*, edited by C. E. Carlson, AIP Conf. Proc. No. 23 (AIP, New York, 1975), p. 575; H. Georgi and D. V. Nanopoulos, Nucl. Phys. **B155**, 52 (1979); **B159**, 16 (1979); L. E. Ibáñez and G. R. Ross, Phys. Lett. B **105**, 439 (1981); M. Olechowski and S. Pokorski, *ibid.* **214**, 393 (1988); D. A. Demir and K. A. Olive, Phys. Rev. D **65**, 034007 (2002).
- [10] F. Borzumati, C. Greub, and Y. Yamada, Phys. Rev. D **69**, 055005 (2004).
- [11] G. Degrassi, P. Gambino, and G. F. Giudice, J. High Energy Phys. **12** (2000) 009; M. Carena, D. Garcia, U. Nierste, and C. E. M. Wagner, Phys. Lett. B **499**, 141 (2001).
- [12] K. Chetyrkin, M. Misiak, and M. Munz, Phys. Lett. B **400**, 206 (1997); **425**, 414(E) (1997); T. Hurth, hep-ph/0106050; C. Greub, T. Hurth, and D. Wyler, Phys. Rev. D **54**, 3350 (1996); K. Adel and Y. Yao, *ibid.* **49**, 4945 (1994); A. Ali and C. Greub, Phys. Lett. B **361**, 146 (1995).
- [13] For a review, see P. Nath, R. Arnowitt, and A. H. Chamseddine, in *Applied N = 1 Supergravity, Lecture Series, 1983* (World Scientific, Singapore, 1984); H. P. Nilles, Phys. Rep. **110**, 1 (1984).
- [14] A. I. Davydychev and J. B. Tausk, Nucl. Phys. **B397**, 123 (1993).
- [15] A. L. Kagan and M. Neubert, Phys. Rev. D **58**, 094012 (1998).
- [16] CLEO Collaboration, T. E. Coan *et al.*, Phys. Rev. Lett. **86**, 5661 (2001).
- [17] K. Chetyrkin, M. Misiak, and M. Münz, Phys. Lett. B **400**, 206 (1997); **425**, 414(E) (1998).
- [18] K. Hagiwara *et al.*, Phys. Rev. D **66**, 010001 (2002).